

REDUCED ORDER MODELS IN UNSTEADY AERODYNAMIC MODELS, AEROELASTICITY AND MOLECULAR DYNAMICS

Earl H. Dowell*, **Kenneth C. Hall***, **Jeffrey P. Thomas***, **Robert E. Kielb***,
Meredith A. Spiker*, **Aiqin Li***, **Charles M. Denegri, Jr.****
***Duke University, **U.S. Air Force SEEK EAGLE Office, Eglin AFB, FL**

Abstract

The state of reduced order modeling of unsteady aerodynamic flows for the efficient calculation of fluid-structure interaction (aeroelasticity) is discussed as well as very recent work on molecular dynamics simulations. Starting with either a time domain or frequency domain computational fluid dynamics (CFD) analysis of unsteady aerodynamic flows, a large, sparse eigenvalue problem is solved. Then, using just a few of the resulting aerodynamic eigenmodes, a Reduced Order Model (ROM) of the unsteady flow is constructed. The aerodynamic ROM can then be combined with a similar ROM for the structure to provide a Reduced Order Aeroelastic Model that reduces computational model sized and cost by several orders of magnitude. Moreover, the aerodynamic and aeroelastic eigenvalue and eigenmode information provides important insights into the physics of unsteady flows and fluid-structure interaction.

As an alternative to the use of aerodynamic eigenmodes, Proper Orthogonal Decomposition (POD) has also been explored. POD is an attractive alternative because of the greater simplicity of calculating POD modes rather than fluid eigenmodes per se. Moreover once the POD modes have been used to construct a Reduced Order Model, this ROM may be used to find a good approximation to the dominant aerodynamic eigenmodes.

After the Hopf Bifurcation (flutter) condition is determined for the fluid-structural system, a novel High Dimensional Harmonic Balance (HDHB) solution method for the fluid (and structural) model(s) proves to be a very

efficient technique for determining limit cycle oscillations in fluid-structural systems.

Examples will be discussed including the limit cycle oscillations (LCO) of the F-16 aircraft and the limit cycle oscillations (LCO) of the Von Karman vortex street behind a cylinder in a cross-flow. The latter is a prototypical example of self-excited fluid oscillations that occur for bluff bodies including wings at high angles of attack. Correlation of theoretical calculations with experiment will also be shown. Finally a discussion of how similar methods may be used for molecular dynamics simulations concludes the paper.

1 Introduction

In this paper the initial focus is on two distinct yet fundamentally related phenomena in unsteady aerodynamics and aeroelasticity. The first is the limit cycle oscillations that may occur in high performance military and civilian aircraft. The other is the wake oscillation and vortex shedding that may occur behind a bluff body and the consequent fluid-structural dynamic interaction. In both cases theoretical modeling and correlation with experiment will be emphasized.

Earlier relevant discussions of these topics include review articles by Dowell and Hall [1] (reduced order aerodynamic modeling), Dowell and Tang [2] (nonlinear aeroelasticity and unsteady aerodynamics) and Dowell, Edwards and Strganac [3] (nonlinear aeroelasticity). Also excellent review articles on these topics have been written by Beran and Silva [4] (reduced order aerodynamic modeling), Lee et al [5] (freeplay and other related structural nonlinearities) and Lucia,

Beran and Silva [6] (reduced order aerodynamic modeling).

Limit cycle oscillations have been observed in the F-16 aircraft and this has motivated much of the work on this subject. Denegri and his colleagues [7-10] have written authoritative articles on results from flight tests and their interpretation in the light of existing mathematical models.

The paper concludes with a discussion of reduced order models in a different physical context, i.e. molecular dynamics simulations.

2 Nonlinear Aeroelastic Response and its Interpretation

To set the stage for our subsequent discussion, first consider Figure 1 which displays a schematic of limit cycle oscillation response as a function of flight speed. Other parameters such as Mach number or altitude might be used in lieu of flight speed, but the latter is as useful a parameter as any for our present purposes.

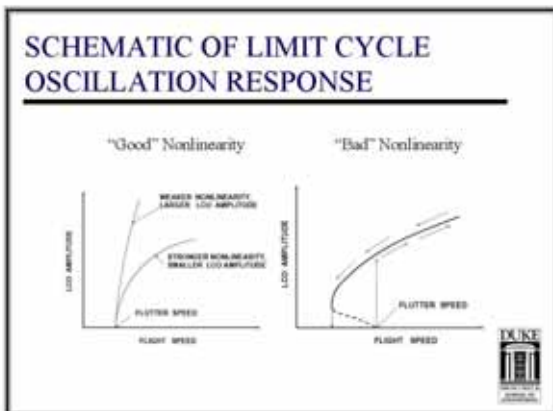


Fig. 1. Schematic of Limit Cycle Oscillation Response

There are two different generic responses shown. One is termed the case of a “good nonlinearity” and for this case there is no steady state limit cycle oscillation (LCO) below the flutter speed. The flutter speed is here defined (and in the present authors' opinion most usefully defined) as the flight velocity at which a dynamically linear (though possibly statically nonlinear) mathematical model would predict the system is dynamically unstable.

Physically it is the velocity one would observe in a flight test or wind tunnel test at which oscillations would begin to grow exponentially with time IF any external dynamic disturbances were sufficiently small. In a mathematical sense such disturbances are assumed to be infinitesimally small, but only a nonlinear dynamic analysis can reveal how small is small enough. Often in experiments the disturbances cannot be kept small enough so that the flutter speed can be precisely determined. As the flight speed continues to increase, the LCO amplitude continues to increase (smoothly) and if the flight speed is decreased the LCO amplitude versus flight speed curve is retraced. Geometric nonlinearities in a low aspect ratio wing structure or a thin skin panel are typical physical sources of good nonlinearities. See Dowell and Tang [2] for a discussion of structural nonlinearities and the relevant literature.

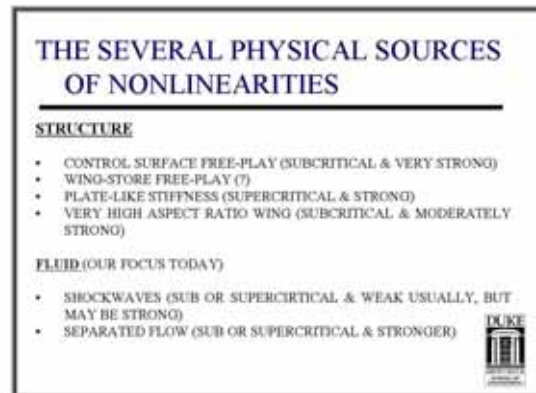


Fig. 2. Several Physical Sources of Nonlinearities

The other generic response shown in Figure 1 is for the case of a “bad nonlinearity”. In this case a limit cycle oscillation (LCO) may occur for flight speeds below the flutter speed IF the external disturbances are large enough. Again a nonlinear analysis is needed to determine how large is large enough and in an experiment one needs to closely control the nature and magnitude of the disturbances. Often such control is a major challenge in an experiment. In the case of a bad nonlinearity, if external disturbances are kept small enough then at the flutter speed there is a sudden jump to a finite amplitude limit cycle oscillation and

with further increases in flight speed the LCO amplitude continues to smoothly increase. However, if the flight speed is decreased, the LCO oscillation will continue to persist to flight speeds below the flutter speed and the aeroelastic system is said to have hysteresis. Freeplay between a control surface and wing structure is a typical source of a bad nonlinearity. See Lee et al [5] and Dowell and Tang [2] for a discussion of freeplay.

Figure 2 lists the principal sources of nonlinearities in aeroelastic systems. They may be inherent in the structure or the aerodynamic flow. They may be further characterized as “good” or “bad” and they may also be sometimes characterized in terms of the amplitude at which such a nonlinearity will become important. If there are several such possible nonlinearities the one that becomes important at the SMALLEST amplitude will generally be dominant for that aeroelastic system. For example, for thin plate-like structures the nonlinearity becomes significant when response amplitudes are of the order of the plate thickness. For freeplay it is when the response amplitudes become of the order of the range of freeplay. When a nonlinearity is important for smaller response amplitudes it is called “strong” and when becomes important for larger response amplitudes it is called “weak”. Also rather than using the terms “good” and “bad”, the more formal (mathematical) terms are sometimes used, “supercritical” and “subcritical”. See Figure 2.

For aerodynamic nonlinearities due to shock motion or separated flow, the response amplitude of amplitude at which such nonlinearities become important is a sensitive function of Mach number, perhaps Reynolds number and aircraft or wing geometry. And indeed these parameters also determine whether the nonlinearity is good or bad. For these reasons and because of the relatively greater difficulty of constructing a nonlinear mathematical model or performing an experiment to study aerodynamic nonlinearities, these are usually a greater challenge to understand and to describe in a compact mathematical model. A corollary of this is that if one wants to design a beneficial nonlinearity

to suppress or at least diminish LCO, structural nonlinearities are usually a much more attractive and robust candidate for this purpose. Finally we emphasize that while LCO may be undesirable, it is usually safer to have LCO than flutter in a flight vehicle or wind tunnel model.

In this paper, the focus will be on aerodynamic nonlinearities due to shock waves and flow separation.

2.1 Some Important Theoretical Ideas

Before presenting representative results, a few fundamental and important theoretical ideas are discussed which form the basis for the methods used to obtain the results to be presented later.

Three ideas are summarized here. The first idea is that of DYNAMIC perturbation theory or as it is sometimes term in the aeroelastic literature, “time linearization”. “Dynamic linearization” would perhaps be a better term. The basis for this idea is the following. Whatever the fundamental fluid or aerodynamic model, be it a potential flow model or an (inviscid) Euler model or a (viscous) Navier-Stokes model, one can always in principle and today in practice do the following. First determine a steady (time independent) flow about (at most) a statically deformed structure. This steady flow solution may itself require a NONLINEAR static or steady flow analysis. Then consider a small dynamic (time dependent) perturbation about this static deformation shape of the structure and the related steady flow field. In terms of the dynamic fluid and structural motion, the governing equations of the mathematical model are LINEAR and all the powerful tools of linear dynamic analysis may be brought into play. This provides a very substantial conceptual and computational simplification for the aeroelastic analysis. And such a model is entirely adequate for determining the flutter boundary of an aeroelastic system. And IF all nonlinearities were “good” rather than “bad”, we would be assured that any limit cycle oscillations that may occur would be at flight speeds higher than the flutter speed. But as we have discussed some nonlinearities are “bad” or “subcritical”. Thus there will be a need for a FULLY

DYNAMICALLY NONLINEAR analysis for some cases, to determine the onset of limit cycle oscillations (LCO) as well as the variation of LCO amplitudes with system parameters.

Traditionally such FULLY DYNAMICALLY NONLINEAR analysis has been conducted by time simulation. But recently Hall and colleagues have developed an alternative method for such analyses based upon the observation that the usual LCO is periodic in time and thus the response can be represented by a Fourier series in time where the unknowns are the amplitudes of a small number of harmonics, typically two or three or even only one. This greatly reduces the computational cost of determining LCO response. The method used is a novel form of the harmonic balance method developed especially for the very high dimensional systems typical of computational fluid dynamic (CFD) models. This has been called the high dimensional harmonic balance (HDHB) method and it is well described by Hall, Thomas and Clark [11], but also in Dowell and Hall [1] and Thomas, Hall and Dowell [12].

The third theoretical idea is use the notion of spatial aerodynamic modes to create an aerodynamic model rather than using local spatial grids typical of traditional CFD codes. Referring back to the first idea of a small dynamic perturbation or time linearization, once such a model exists it is natural to find its eigenmodes and then reconstitute the CFD model in terms of such eigenmodes. For many years aeroelasticians have done this for complex structural models and with great success. So it may be somewhat surprising that this has only been done relatively recently for aerodynamic models. But the reason for this is not far to seek. Finding the eigenmodes of a typical CFD code is a far more difficult task than for a typical finite element structural model and the interpretation of such eigenmodes is more subtle. For a more in depth discussion see Dowell and Hall [1]. Here we simply note that the eigenvalues of such eigenmodes are complex numbers representing the frequency and damping in each aerodynamic mode and for an unbounded fluid domain the eigenvalues are continuous rather than discrete. Nevertheless for time linearized models this idea has been used

with great success to determine flutter boundaries using the Euler and Navier-Stokes equations for the fluid. It typically reduces computational costs by a factor of 100 to 10,000 depending on the particulars of the aeroelastic system. Most recently the use of Proper Orthogonal Decomposition to construct modal basis vectors has been shown to be a relatively simple and effective approach and is currently the method of choice.

To use the second and third ideas in combination is currently a subject of research. Yet another attractive idea is to use (POD) aerodynamic modes in combination with system identification methods to construct a reduced order FULLY NONLINEAR REDUCED ORDER MODEL. See the paper by Lucia, Beran and Silva [6] and also the paper by Attar, Dowell, White and Thomas [13].

2.2 The F-16 Aircraft: Flutter and Limit Cycle Oscillations

This discussion of the F-16 aircraft relies substantially on the paper by Thomas, Dowell, Hall and Denegri [14] as well as more recent as yet unpublished work of these same colleagues. The challenge is that the F-16 may undergo limit cycle oscillations (LCO) and there are many possible stores that can be carried by this aircraft and hence its structural dynamic, unsteady aerodynamic and aeroelastic characteristics may change from one store configuration to another. To date flight testing has been used to determine the LCO response of the F-16 configurations and this is very expensive and time consuming. Yet there has not been a reliable theoretical method to predict LCO. Here one approach is discussed that has proven to be useful and the results obtained are encouraging.

In our work to date we have modeled the aerodynamic flow around the wing, but only used highly simplified geometries to represent the aerodynamics of the stores per se. The structural characteristics of the wing plus store are fully accounted for by a dynamically linear structural model in terms of the natural modes as derived from a finite element structural model. Both Euler based and Navier-Stokes

based aerodynamic CFD codes have been used. But for this configuration we only show results from the Navier-Stokes fluid model as the Euler model does not appear adequate for this configuration at the Mach numbers and Reynolds numbers of interest.

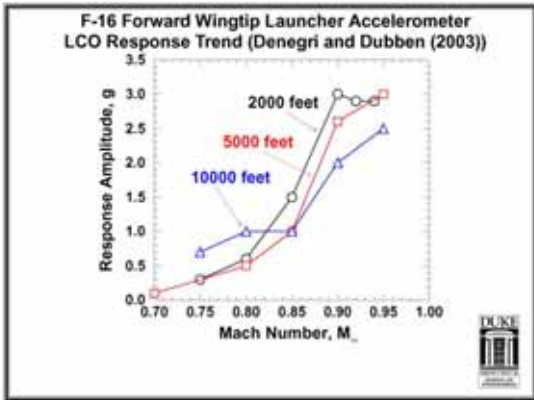


Fig.3. F-16 Forward Wingtip Launcher Accelerometer LCO Response Trend (Denegri et al)

Figure 3 shows the measured dynamic response of the aircraft in terms of acceleration at a forward position on the wingtip launcher as a function of Mach number at several fixed altitudes. The results are not especially sensitive to altitude over the range shown. For $M=0.9$ LCO seems clearly indicated and for M less than 0.75 it appears there is no LCO. For this configuration no appreciable hysteresis was seen, i.e. it appears that there is a “good nonlinearity”. The question arises then, what is the flutter Mach number? As with beauty, the flutter Mach number may be at least to some degree in the eye of the beholder. Because of atmospheric disturbances and perhaps pilot induced disturbances as well, the external excitations are not completely controlled and appear to be sufficiently large to mask a precise determination of the flutter Mach number. It appears to be somewhere in the range of $M=0.8$ to 0.9 . As we will see, in the theory any external disturbance can be suppressed, and a precise determination of the flutter Mach number is obtained that falls in this range of Mach number, i.e. $M = 0.8$ to 0.9 .

A summary of the theoretical model used to compute the flutter Mach number per se

is now described. The governing aeroelastic equation is the usual Lagrangian formulation except the aerodynamic model may be dynamically linear or nonlinear depending on our purpose and what we wish to determine from the model, i.e. flutter only or LCO response as well. The structural modes were determined from a NASTRAN finite element analysis. The aerodynamic generalized forces depend parametrically on the aeroelastic frequency, modal displacement amplitudes, Mach number, Reynolds number, any mean or static angle of attack and altitude.

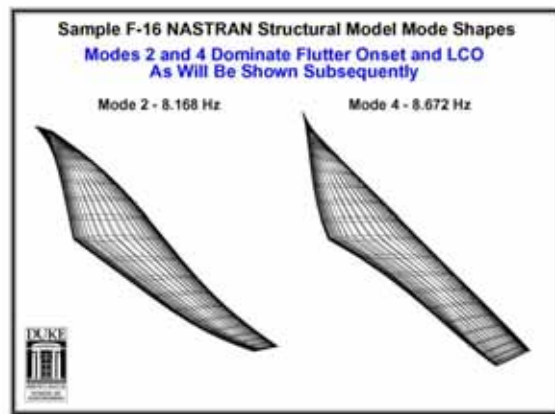


Fig. 4. Sample F-16 NASTRAN Structural Model Mode Shapes

The generalized aerodynamic forces are nonlinear functions of the structural modal amplitudes when undertaking a LCO analysis, but are linear functions (the analysis is time linearized) when only a flutter analysis is performed. Of course the flutter point may be determined by the fully nonlinear analysis used for LCO, but it is certainly less expensive and usually more insightful to use a dynamically linear analysis for predicting the flutter Mach number per se. The results in this paper were obtained by first using a dynamically linear analysis to determine the flutter Mach number and then a fully nonlinear dynamical analysis to determine LCO.

Figure 4 shows the two most important structural modes which contribute to the flutter mode and the LCO response. Note these modes are antisymmetric and have closely spaced natural frequencies.

A novel high dimensional harmonic balance procedure (HDHB) used to calculate a solution to the aerodynamic CFD model. Expanding the solution in a Fourier Series in time, one seeks to find the coefficients of the Fourier Series. When the underlying CFD model is fully nonlinear dynamically, there is nonlinear coupling among these Fourier coefficients. It is noted that there is unique relationship (transformation) between these Fourier coefficients and the solution at certain discrete times over ONE period of the LCO. For technical reasons it is simpler to determine the solution at these discrete times directly. For a more in depth discussion of the HDHB methodology, see Hall et al [11] or Thomas et al [12].

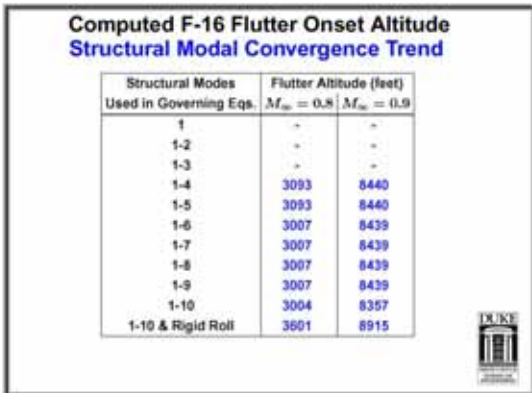


Fig.5. Computed F-16 Flutter Onset Altitude Structural Modal Convergence Trend

2.3 Flutter and LCO Calculations:

Figure 5 shows the altitude at which flutter is calculated to occur at two different Mach numbers, $M = .8$ and $.9$. Also shown are results for various combinations of structural modes retained in the aeroelastic model. Note the symmetric structural modes, i.e. 1, 3, 5, etc. make no detectable contribution to the flutter mode and that the lowest two antisymmetric structural modes, i.e. 2 and 4, dominate the flutter solution. There is a discernible, if modest, effect on flutter due to the rigid body roll mode.

Figure 6 shows the flutter boundary as a plot of altitude versus Mach number. Also shown in the inset box is the modal amplitude

ratio of the two dominant modes showing both the in-phase (real) and out of phase (imaginary) components. The flutter frequency does not change much with altitude and is near the two closely spaced resonant frequencies of the two dominant structural modes.

The HDHB LCO solution methodology is as follows. An amplitude of a prominent structural mode is chosen and the solution procedure determines the amplitude of all other structural modes, the frequency of the LCO and the Mach number at which those LCO amplitudes and frequency will occur. The solution method is basically solving a NONLINEAR eigenvalue problem by driving the characteristic determinant of the aeroelastic model to zero.

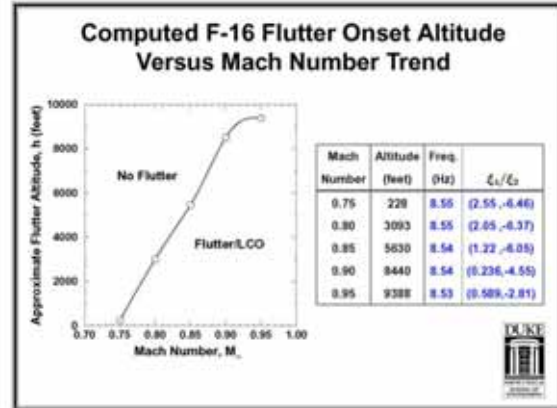


Fig. 6. Computed F-16 Flutter Onset Altitude vs. Mach Number Trend

Figure 7 shows the LCO results from the theoretical model compared to the results from flight test. As may be seen the theoretical model predicts a precise flutter Mach number because all external disturbances have been suppressed. Also the theoretical model does well in predicting the maximum LCO response and the range of Mach number where LCO is seen in the flight test. It would be of interest to include some representation of the external disturbances in the calculation if we had an accurate knowledge of what they are. This might be best done by using the HDHB analysis to compute a (nonlinear) transfer function for the aeroelastic model and using a power spectral density representation of a random gust. Finally it is noted that the theoretical model predicts

correctly the critical (antisymmetric) structural modes and the observed LCO frequency.

Perhaps it bears some emphasis to note that in fact the LCO predicted is the result of the onset of flutter which is then followed by LCO as the aircraft flies beyond the flutter boundary. No hysteresis is seen in the present calculations. Interestingly hysteresis was observed in some earlier calculations using the Euler fluid model, however the Euler model predicts LCO behavior that is quite different from the Navier-Stokes model and is in poorer agreement with the flights test measurements. Hence these results are not shown.

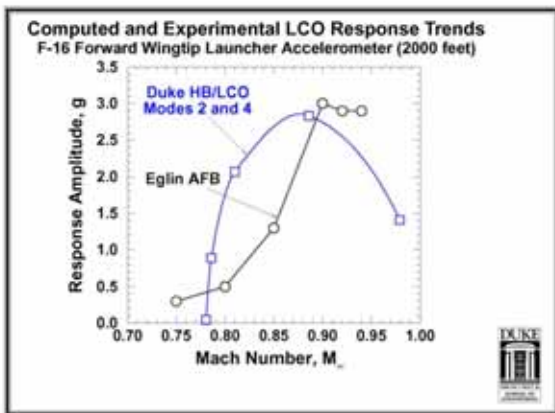


Fig. 7. Computed and Experimental LCO Response Trends

The main conclusions of the F-16 study are that the HDHB/LCO solution technique works well and is the only method to date to predict LCO for the F-16. The LCO response levels correlate well with experiment and the computational times are far less than any other methods proposed to date.

2.4 Unsteady Flow About a Circular Cylinder in a Cross-Flow

Another class of unsteady aerodynamic and nonlinear aeroelastic phenomena is the study of flow around a bluff body. Of course streamlined bodies become bluff bodies if placed at a sufficiently high angle of attack. Thus buffeting of aircraft at high angles of attack, such as wing drop or abrupt wing stall as most recently seen on the F-18 but also as seen over many years on other aircraft, as well as the flow around ships

all are important examples of this class. Here we consider the classic example of the class, i.e. the famed Von Karman vortex street that occurs behind a circular cylinder in cross flow at sufficiently high Reynolds number. As an aside, in his autobiography Theodore Von Karman notes that in France the Von Karman vortex street is known as Bernard Boulevard and in Germany as Prandtl Strasse. Whatever the name it is a very interesting nonlinear dynamic unsteady flow. The work described here has been briefly discussed by Thomas et al [15-17]. The prior experiments were reported by Anagnostopoulos and Bearman [18].

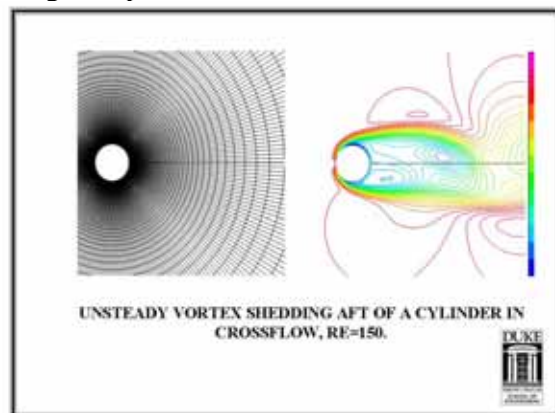


Fig. 8. Unsteady Vortex Shedding Aft of a Cylinder in Crossflow, RE=150

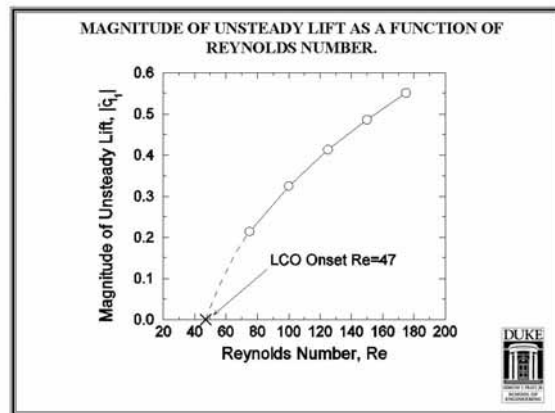


Fig. 9. Magnitude of Unsteady Lift as a Function of Reynolds Number

Figure 8 shows the circular cylinder geometry, the CFD grid and a typical flow pattern of total pressure contours for vortex shedding behind the cylinder.

- **Stationary Cylinder:** Even if the cylinder is stationary, the flow may begin to oscillate above a critical Reynolds number, $Re_{critical}$. Based upon cylinder diameter, $Re_{critical}=47$. Above this Re there is a limit cycle oscillation of the flow alone, using the language of this paper. Thus in Figure 9 the magnitude of the unsteady lift is shown as a function of Re . Unfortunately there are no experimental data to compare to the theoretical results of Figure 9. However, for the range of Re shown, the flow oscillation is dominated by a single harmonic of a certain frequency (Strouhal number) that is in good agreement with previous experiments (not shown here).

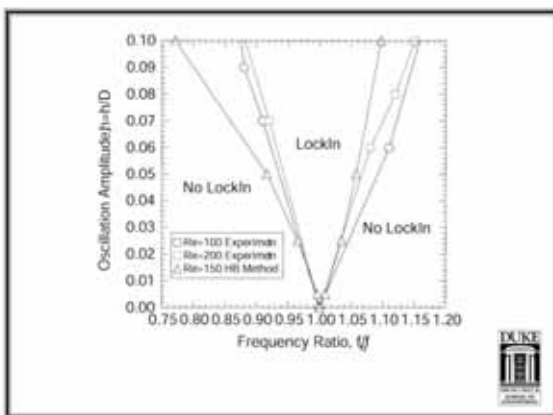


Fig. 10. Oscillation Amplitude vs. Ration of Strouhal Frequency of Wake to Prescribed Frequency of Cylinder Motion

- **Cylinder with Prescribed Motion:** When the cylinder is given a motion of a prescribed amplitude and frequency, and if this frequency is sufficiently near the Strouhal frequency of the flow (the frequency of the flow LCO when the cylinder is not moving), then the flow will oscillate with the prescribed frequency and not the flow Strouhal frequency. In Figure 10, results are shown for this so called “lock-in” range in terms of cylinder frequency normalized by the Strouhal frequency versus amplitude of cylinder motion. The agreement between the present

theoretical results and prior experiments is very good for low amplitudes and less good at higher amplitudes where higher harmonics not included in the analysis are thought to be more important.

- **Cylinder Free to Move/Aeroelastic Cylinder:** If the cylinder is spring mounted so that it is free to move and dynamically interact with the oscillating flow, then even more interesting responses arise. Now an aeroelastic LCO is possible and indeed occurs. Figure 11 shows the LCO amplitude of the cylinder response normalized by the cylinder diameter versus Reynolds number. This self-excited response is present most prominently in the lock-in range and the frequency of the response is very nearly the natural frequency of the structure, i.e. the resonant frequency of the cylinder mass on the spring mount. Results are shown from previous experiments and also from the present analysis. Theoretical results are shown for various numbers of harmonics retained in the analysis to illustrate the good harmonic convergence of the HDHB analysis. The analysis agrees very well with the main features of the experimental results, i.e. the abrupt jump in LCO amplitude that occurs at $Re=105$ as well as the smoother decrease of the LCO amplitude with Re as the Re increases to about 130. It is interesting to note that the analysis predicts two possible LCO amplitudes over a smaller range of Re from about $Re=125$ to 130. It is thought, but not yet conclusively shown, that the smaller LCO amplitude in this range of Re corresponds to an LCO which is itself unstable. If so, then this LCO also shows hysteresis in this range of Re . Finally the underprediction of the largest LCO amplitudes shown in Figure 31 may be a result of only using one harmonic in the structural analysis even though higher harmonics were included in the fluid model.

The principal conclusion drawn from this example is that unsteady and unstable

aerodynamic flows may also be treated by the methods that have been developed and discussed here. Moreover bluff as well as aerodynamic streamlined bodies and their aeroelastic behavior may be studied by these new methods.

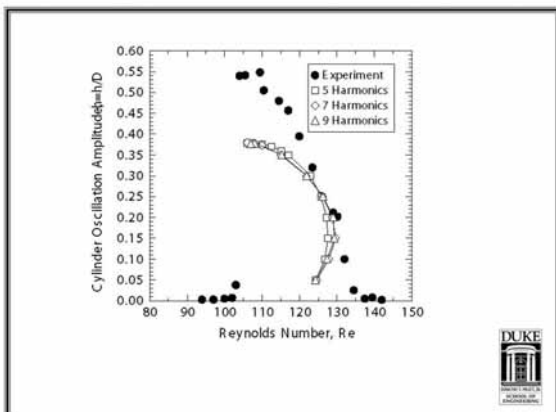


Fig. 11. LCO Amplitude vs. Reynolds Number

3 Modal Reduction of Mathematical Models of Biological Molecules

A detailed study has been undertaken [19] of modal reduction based on either linear normal mode (LNM) analysis or proper orthogonal decomposition (POD) for modeling a single -D-glucopyranose monomer as well as a chain of monomers. Also a modal reduction method combining POD and component modal synthesis (CMS) has been developed. The focus of this study is to determine to what extent these methods can reduce the time and cost of molecular modeling and simultaneously provide the required accuracy. It has been demonstrated that a linear reduced order model (ROM) is valid for small amplitude excitation and low frequency excitation. It is found that a nonlinear ROM based on POD modes provides a good approximation even for large excitation while the nonlinear ROM using linear eigenmodes as the basis vectors is less effective for modeling molecules with a strong nonlinearity. The ROM based on CMS using POD modes for each component also gives a good approximation. With the reduction in the dimension of the system using these methods the computational time and cost can be reduced significantly.

3.1 Physical Context

Biomolecular motions involve a large number of atoms and take place over a great range of time and length scales. Moreover, because of the existence of high frequency motions, the usual time step in a molecular dynamics simulation is around 1 femtosecond. These characteristics make a numerical molecular dynamic simulation a computationally intensive task. There is a clear need to reduce the cost of the computation. Modal reduction methods described here are directed toward that end.

A key challenge for constructing low-dimensional models for complex physical systems is the choice of basis vectors. In this research two kinds of subspaces are considered, linear normal mode (LNM) and proper orthogonal decomposition modes (POD). The POD method is a procedure for extracting modal information from a set of data obtained in experiments or numerical simulations, thus providing an optimal basis for modal reduction.

The application of modal analysis to molecular dynamics first appeared in the early 1980s. In [20] the author shows that multiple minima exist in proteins and the harmonic (quadratic) approximation of the potential energy is in question. Paradoxically, in [21] it is proven that the very low-frequency normal modes make the major contributions to the conformational fluctuations at thermal equilibrium and the author argued that this fact justifies the use of very-low-frequency normal modes to describe the most significant conformational dynamics of proteins. The use of traditional normal modes is still under study today. As an alternative to traditional normal modal analysis, POD has been introduced in molecular dynamics. In [22] the authors applied both normal modal analysis and principal component analysis to the dynamics of BPTI and the results show that the first principal component makes an overwhelmingly large contribution to the total mean-square fluctuation and represents the transitions between energy minima or static equilibria. For more examples, see references [23-27]. The results of these papers support the use of modal reduction in computational biology.

However, so far in molecular dynamics most reduced order models using normal modes or POD are assumed to be linear around the static equilibrium state or conformation. The study of a nonlinear reduced order model is rarely considered. In [19] normal modes and POD modes are used to construct linear and nonlinear reduced order models for a α -D-glucopyranose monomer to determine if modal reduction can provide a good approximation to the original system and can improve the efficiency of computation in molecular dynamics. This is a continuation of our previous studies that mainly used linear models [28].

In addition, a reduced order model based on POD and component modal synthesis (CMS) is also constructed. As is well known, component modal synthesis can be advantageous in modeling large systems. For biological molecules, the dimension of the system is very high. The calculation of proper orthogonal modes (POM) for the entire system is very expensive since the correlation matrix is so big. And also the accuracy may be in doubt when solving a large eigenvalue problem. Thus, CMS is another attractive option. To demonstrate the utility of this method, the simulation of a ten-monomer amylose chain is carried out.

3.2 Method and Discussion

The chemical formula of α -D-glucopyranose is $C_6H_{12}O_6$. It includes 24 atoms and has a six-member ring structure with one side-group. The latest version [29] of the parameters for the semi-empirical potential energy is used in the simulations here.

The schematic diagram of a α -D-glucopyranose chain with an Atomic Force Microscope (AFM) attached is shown in Figure 12. Assume the AFM is attached to atom k and moves along the z -direction. In matrix form the equations of motion are given by

$$\mathbf{M} \ddot{\mathbf{x}} + \mathbf{C} \dot{\mathbf{x}} - \mathbf{F}_N + \mathbf{F}_e = k_s B(t) \delta(i-k) \quad (1)$$

where \mathbf{x} is the position vector for the atoms, \mathbf{M} is a diagonal matrix of the atomic mass, \mathbf{F}_e is the

force due to the AFM and \mathbf{F}_N is the force due to the potential energy which describes atom interactions. The equation for the reduced order models (ROM) is the projection of this equation to the subspace spanned by LNM or POM.

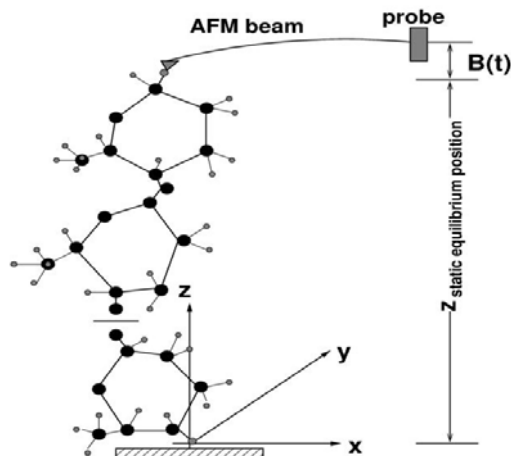


Fig. 12. Schematic Diagram for Stretching of the Molecule by an AFM

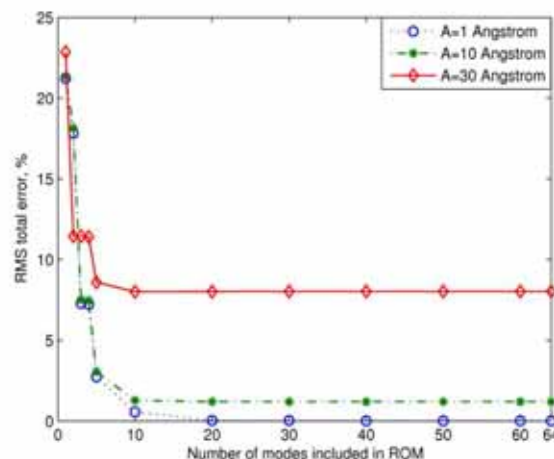


Fig. 13. Total RMS Error vs. Number of Eigenmodes for Different Excitation Amplitudes Using the Linear ROM $f=100\text{GHz}$

3.3 Linear ROM Results

Figure 13 shows the total rms error compared to the exact solution vs. the number of modes included in the linear ROM for different excitation amplitudes with the frequency of $f=100\text{GHz}$. The total rms error is defined to be the mean square of the error of the rms amplitudes for all the atoms calculated by the

ROM compared to the original equations. The total error decreases as the number of modes included in the linear ROM increases and eventually reaches a constant value which accounts for the difference between the fully linear model and the original nonlinear system. As the excitation amplitude increases, this difference gets larger.

3.4 Nonlinear ROM Results

Figure 14 shows the total rms error vs. the number of LNM or POM in the nonlinear ROM. It is found the results from the ROM based on LNM converge to the exact solution much more slowly than the results obtained from the ROM with POM as the basis. For the LNM, the results agree well with the exact solution when full model is used but the error increases significantly even if only a few high frequency modes are omitted in the ROM. This is probably because linear eigenmodes are no longer invariant manifolds. Reduced order models based on LNM cannot capture the essential dynamics by simply truncating the high frequency modes. This is similar to the case reported in [30].

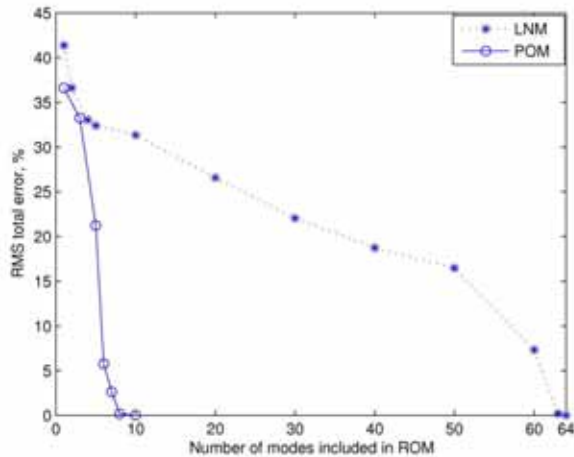


Fig. 14. Total RMS Error vs. Number of LNM or POM Included in the Nonlinear ROM. $A=1\text{\AA}$ and $f=100\text{GHz}$

3.5 Reduction in Computational Time

With the ROM, the computational time and cost can be significantly reduced in two ways: (1) by decreasing the number of system variables

which characterize the system dynamics and (2) by increasing the computational time step. For the linear models both ways contribute to the increase of computational efficiency. For nonlinear reduced order models the efficiency is achieved mainly by increasing the time step, see Figure 15 for an example. Figure 15 shows the computational time for the POD/CMS ROM relative to the original full time marching model vs. the logarithm of the time step used in the simulations. In the plot the relative computational time is defined to be the ratio of the computational time for the ROM to that of the original system. The computational time of the original system is that for time marching a solution with a time step of $2 \times 10^{-3}\text{ps}$, which is the maximum allowable time step for the original system. It turns out that the computational time and cost of the ROM can be significantly reduced (by a factor of up to 10) by increasing the time step without changing the solution accuracy. Also it is noted that the models with lower dimension have a slightly smaller relative computational time.

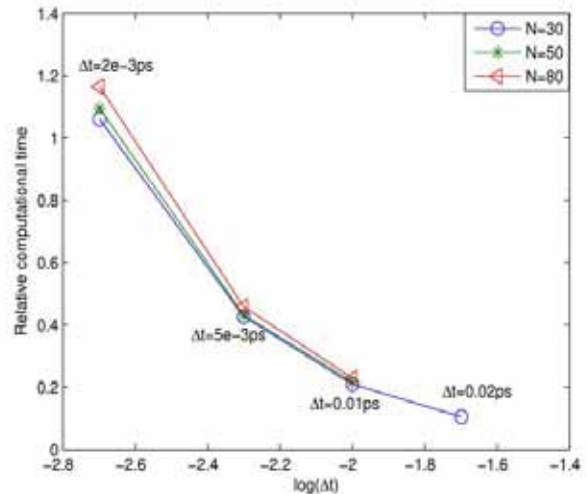


Fig. 15. Ratio of Computational Time for ROM (POD and CMS) model to that of a Time Marching Solution Vs. the Chosen Numerical Time Step for Different Number of Modal Coordinates retained, N , in the whole system. $A=1\text{\AA}$ and $f=20\text{GHz}$

3.6 Conclusions

A detailed study of modal reduction based on LNM and POM has been carried out in

modeling a α -D-glucopyranose monomer and also a chain of monomers under harmonic AFM base excitation. It has been demonstrated that the linear reduced order model (ROM) is valid for small amplitude excitation and low frequency excitation. The nonlinear reduced order model with LNM as the basis vectors is less useful in modeling the molecules with a strong nonlinearity. Fortunately, the nonlinear reduced order model based on POM provides a good approximation even for large amplitude or high frequency excitation. Also it is important to note that the POM model obtained in one case for a given amplitude of excitation is applicable for a wide range of excitation amplitudes.

A reduced order model based on component modal synthesis using POM for each component can also be constructed. Although the POM for each component is calculated from the full model simulation, CMS makes the eigenvalue problem of the correlation matrix more tractable and more efficient. Since there are many complicated and large biological molecules in the nature, the combination of CMS and POD may provide a useful method for modeling their dynamic behavior.

With the reduced order system, the computational time and cost can be significantly reduced by a factor of ten or even a hundred depending on the external excitations and whether the linear or nonlinear model is used in the simulation. Therefore, modal reduction is a possible, effective way to decrease the computational time and cost of a molecular dynamics simulation.

4 References

- [1] Dowell EH, Hall KC (2001) Modeling of Fluid-Structure Interaction, Annual Review of Fluid Mechanics 33: 445-90
- [2] Dowell EH, Tang D (2002) Nonlinear Aeroelasticity and Unsteady Aero-Dynamics. AIAA Journal 40(9): 1697-1707
- [3] Dowell EH, Edwards JW, Strganac T (2003) Nonlinear Aeroelasticity. Journal of Aircraft 40(5): 957-876
- [4] Beran P, Silva W (2001) Reduced-Order Modeling: New Approaches for Computational Physics. AIAA Paper 2001-0853, 39th Aerospace Sciences Meeting and Exhibit, January, Reno, NV
- [5] Lee BHK, Price SJ, Wong YS (1999) Nonlinear Aeroelastic Analysis of Airfoils: Bifurcation and Chaos. Progress in Aerospace Sciences 5, (3): 205-334.
- [6] Lucia D, Beran P, Silva W (2004) Reduced Order Modeling: New Approaches for Computational Physics. Progress in Aerospace Sciences 40: 51-117
- [7] Denegri CM Jr, (1997) Correlation of Classical Flutter Analyses and Nonlinear Flutter Responses Characteristics. International Forum on Aeroelasticity and Structural Dynamics, June, Rome, Italy
- [8] Denegri CM Jr, Cutchins MA (1997) Evaluation of Classical Flutter Analysis for the Prediction of Limit Cycle Oscillations. AIAA Paper 97-1021, AIAA/ASME/ASCE/AHS/ASC Structures, Structural Dynamics, and Materials Conference and Exhibit, 38th, and AIAA/ASME/AHS Adaptive Structures Forum, April 7-10, Kissimmee, Florida
- [9] Denegri CM Jr, (2000) Limit Cycle Oscillation Flight Test Results of a Fighter with External Stores. Journal of Aircraft 37(5): 761-769
- [10] Denegri CM Jr, Johnson MR (2001) Limit Cycle Oscillation Prediction Using Artificial Neural Networks. Journal of Guidance, Control, and Dynamics 24(5): 887-895, 2001.
- [11] Hall KC, Thomas JP, Clark WS (2002) Computation of Unsteady Nonlinear Flows in Cascades Using a Harmonic Balance Technique. AIAA Journal 40(5): 879-886
- [12] Thomas JP, Dowell EH, Hall KC (2004) Modeling Viscous Transonic Limit Cycle Oscillation Behavior Using a Harmonic Balance Approach," Journal of Aircraft 41(6): 1266-1274
- [13] Attar PJ, Dowell EH, White JR, Thomas JP (2005) A Reduced Order Nonlinear System Identification Methodology," Submitted to AIAA Journal
- [14] Thomas JP, Dowell EH, Hall KC, Denegri CM Jr (2004) Modeling Limit Cycle Oscillation Behavior of the F-16 Fighter Using a Harmonic Balance Approach. AIAA Paper 2004-1696, Presented at the 45th AIAA/ASME/ASCE/AHS/ASC Structures, Structural Dynamics and Material Conference and Exhibit, April 19-22, Palm Springs, CA
- [15] Thomas JP, Kielb RE, Hall KC (2003) Non-Synchronous Vibrations of Turbomachinery Airfoils. AFOSR Turbulence and Rotating Flows Annual Review, Destin, FL
- [16] Thomas JP, Hall KC, Spiker MA (2004) Non-Synchronous Vibrations of Turbomachinery Airfoils. AFOSR Turbulence and Rotating Flows Annual Review, Denver, CO
- [17] Carlson HA, Feng JQ, Thomas JP, Kielb RE, Hall KC, Dowell EH (2005) Computational Models for Nonlinear Aeroelasticity. AIAA Paper 2005-1085, 43rd AIAA Aerospace Sciences Meeting, January 10-13, Reno, NV

- [18] Anagnostopoulos P, Bearman PW (1992) Response Characteristics of Vortex-Excited Cylinder at Low Reynolds Numbers. *Journal of Fluids and Structures*, 6: 39-50
- [19] Li A, Dowell EH (2006) Modal Reduction of Mathematical Models of Bio-logical Molecules. *Journal of Computational Physics*, 211: 262-288
- [20] Elber R, Karplus M (1987) Multiple Conformational States of Proteins: A Molecular Dynamics Analysis of Myoglobin. *Science*, 235(4786): 318-321
- [21] Go, N, (1990) A Theorem on Amplitudes of Thermal Atomic Fluctuations in Large Molecules Assuming Specific Conformations Calculated by Normal Mode Analysis. *Biophysical Chemistry*, 35: 105-112
- [22] Hayward S, Kitao A, Go N (1994) Harmonic and Anharmonic Aspects in the Dynamics of BPTI: A Normal Mode Analysis and Principal Component Analysis. *Protein Science*, 3: 936-943
- [23] Hayward S, Go N (1995) Collective Variable Description of Native Protein Dynamics. *Annual Review of Physical Chemistry*, 46: 223-250
- [24] Brooks BR, Janezic D, Karplus M (1995) Harmonic Analysis of Large Systems I: Methodology. *Journal of Computational Chemistry*, 16(12): 1522-1542.
- [25] Brooks BR, Janezic D, Karplus M (1995) Harmonic Analysis of Large Systems II: Comparison of Different Protein Models. *Journal of Computational Chemistry*, 16(12): 1543-1553
- [26] Janezic D, Venable RM, Brooks BR (1995) Harmonic Analysis of Large Systems III: Comparison with Molecular Dynamics. *Journal of Computational Chemistry*, 16(12): 1554-1566
- [27] Kitao A, Go N (1999) Investigating Protein Dynamics in Collective Coordinate Space. *Current Opinion in Structural Biology*, 9: 164-169
- [28] Tang D, Li A, Attar P, Dowell E H (2004) Reduced Order Dynamic Model for Polysaccharides Molecule Attached to an Atomic Force Microscope. *Journal of Computational Physics*, 201: 723-752
- [29] Kuttel M, Brady JW, Brady KJ (2001) Carbohydrate Solution Simulations: Producing a Force Field with Experimentally Consistent Primary Alcohol Rotational Frequencies and Populations. *Journal of Computational Chemistry*, 23(13): 1236-1243
- [30] Touze C, Thomas O, Chaigne A (2004) Hardening/Softening Behavior in Nonlinear Oscillations of Structural Systems Using Nonlinear Normal Modes. *Journal of Sound and Vibration*, 273: 77-101
- third party material included in their paper, to publish it as part of their paper. The authors grant full permission for the publication and distribution of their paper as part of the ICAS2008 proceedings or as individual off-prints from the proceedings.

Copyright Statement

The authors confirm that they, and/or their company or institution, hold copyright on all of the original material included in their paper. They also confirm they have obtained permission, from the copyright holder of any